

# A new dissipation term for finite-difference simulations in Relativity

Daniela Alic, Carles Bona and Carles Bona-Casas

Departament de Física, Universitat de les Illes Balears  
Institute for Applied Computation with Community Code (IAC<sup>3</sup>).

**Abstract.** We present a new numerical dissipation algorithm, which can be efficiently used in combination with centered finite-difference methods. We start from a formulation of centered finite-volume methods for Numerical Relativity, in which third-order space accuracy can be obtained by employing just piecewise-linear reconstruction. We obtain a simplified version of the algorithm, which can be viewed as a centered finite-difference method plus some 'adaptive dissipation'. The performance of this algorithm is confirmed by numerical results obtained from 3D black hole simulations.

## 1. Introduction

In a recent paper (Alic *et al* 2007), we presented a centered finite-volume (CFV) method for black-hole simulations in numerical relativity. This method is a variant of the well known local-Lax-Friedrichs approach (LLF), which is currently being used in computational fluid dynamics (including magneto-hydrodynamics). For a specific choice of the parameters, this method can be written as a piecewise-fourth-order finite-difference (FD) algorithm plus a piecewise-third-order accurate artificial dissipation, with automatically tuned local coefficient. The piecewise prefix comes from the slope limiters that are incorporated in order to deal with shocks or other discontinuities.

Current black hole simulations in Numerical Relativity use instead centered FD algorithms combined with a numerical dissipation term of the Kreiss-Oliger type (Gustafson *et al* 1995). This combination can be interpreted as a single numerical scheme with built-in dissipation, which can be tuned by a single parameter. In most numerical relativity simulations, where only smooth profiles are dealt with, this has shown to be an efficient computational approach. In some black hole simulations, however, the required amount of dissipation varies from the inner to the outer regions, so this approach is lacking some flexibility.

Our main point is that, as far as the slope limiters are not required, the FV algorithm which we developed can be expressed also as a fourth-order centered FD algorithms combined with a local dissipation term which is automatically adapted to the requirements of the either interior or exterior black hole regions.

## 2. The Centered Finite-Volume Method in a Flux-Splitting Approach

We consider the Einstein field equations written as a system of balance laws

$$\partial_t u + \partial_k F^k(u) = S(u), \quad (1)$$

where the Flux terms  $F$  and the Source terms  $S$  depend algebraically on the array of dynamical fields  $u$ . We will consider first the one-dimensional case. In a regular finite difference grid, we choose the elementary cell to be the interval  $(x_{i-1/2}, x_{i+1/2})$  centered in the grid point  $x_i$ . The resulting discrete scheme is given by

$$u_i^{n+1} = u_i^n - \frac{\Delta t}{\Delta x} [ F_{i+1/2}^x - F_{i-1/2}^x ] + \Delta t S_i. \quad (2)$$

This general algorithm requires the prescription of the interface fluxes  $F_{i\pm 1/2}^x$ . We will use linear reconstruction: the dynamical fields will be modelled as piecewise linear functions in each cell.

Our CFD method (Alic *et al* 2007) is based on the flux-splitting approach, in which the information is evaluated at the grid nodes, selecting the components of the flux that will propagate in each direction. In every grid point, the flux can then be splitted into two components

$$F_i^\pm = F_i \pm \lambda_i u_i, \quad (3)$$

where  $\lambda$  is the maximum characteristic speed at the specific grid point. In this way, we will have the freedom to choose a different slope for each component, which will allow us to improve the space accuracy.

Then we will consider at each interface two one-sided (left and right) predictions from the neighboring points:

$$F_L^+ = F_i^+ + \frac{1}{2} \sigma_i^+, \quad F_R^- = F_{i+1}^- - \frac{1}{2} \sigma_{i+1}^-, \quad (4)$$

where  $\sigma$  is the slope of the selected flux component in the corresponding cell. The interface flux is obtained by recombining both predictions

$$F_{i+1/2} = \frac{1}{2} (F_L^+ + F_R^-). \quad (5)$$

### 3. Third-order-accurate Dissipation Formula

Let us write the prescription for the slopes of the flux components generically as

$$\sigma_i^+ = a \sigma_i^L + (1-a) \sigma_i^R, \quad \sigma_i^- = b \sigma_i^L + (1-b) \sigma_i^R, \quad (6)$$

where  $a$  and  $b$  are slope coefficients, and we have noted for short

$$\sigma_i^L = F_i^\pm - F_{i-1}^\pm, \quad \sigma_i^R = F_{i+1}^\pm - F_i^\pm. \quad (7)$$

We determine the specific values of the slope coefficients which allow third order accuracy, by inserting the slope formulae in the CFV method. Comparing the final algorithm with the standard fourth order finite difference method, one obtains the values  $a = 1/3$ ,  $b = 2/3$  for the slope coefficients. If no slope limiters are implemented, the derivative of the flux can be expressed in closed form as

$$D_x(F_i) = \frac{1}{12\Delta x} [-F_{i+2} + 8 F_{i+1} - 8 F_{i-1} + F_{i-2}] + Dis(F_i), \quad (8)$$

where the first part of the formula is just the centered fourth-order FD algorithm and the second part is the new dissipation term:

$$Dis(F_i) = \frac{1}{12\Delta x} [\lambda_{i+2} u_{i+2} - 4 \lambda_{i+1} u_{i+1} + 6 \lambda_i u_i - 4 \lambda_{i-1} u_{i-1} + \lambda_{i-2} u_{i-2}]. \quad (9)$$

We test the stability and convergence of the resulting algorithm in the Gauge Wave Test (Fig. 1), one of the standard tests for Numerical Relativity (Alcubierre *et*

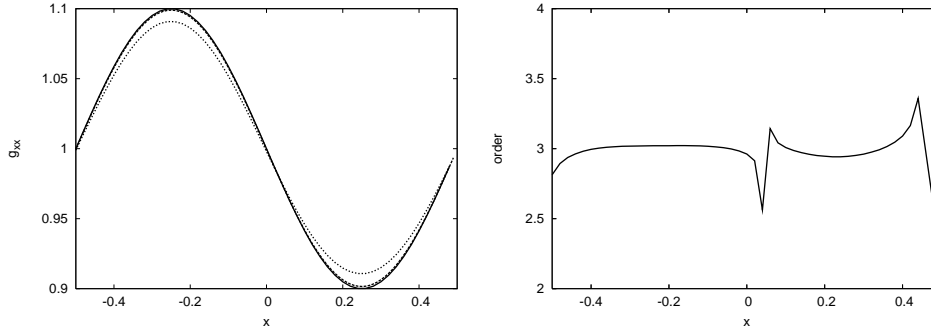


**Figure 1.** 3D Gauge-Wave test simulations. The profiles in the left panel are plots of the metric component  $g_{xx}$  for three resolutions ( $\Delta x = 0.02, 0.01, 0.005$ ) after 100 crossing times; the last two almost coincide. The right panel shows the local convergence rate, calculated by comparing the two higher resolutions with the exact solution, confirming third-order convergence.

al 2004). The plots show that the resulting amount of dissipation is actually very small and confirm third-order convergence. Note, however, that in this case all the local  $\lambda$  coefficients are equal to one, so the new dissipation term coincides with the Kreiss-Oliger one for a specific value of its global coefficient.

#### 4. The 3D Black Hole

The dissipation algorithm presented above can be easily extended to the 3D case:

$$\begin{aligned}
 Dis(F_{i,j,k}^x) = & \frac{1}{12\Delta x} [ \lambda_{i+2,j,k}^x u_{i+2,j,k} - 4 \lambda_{i+1,j,k}^x u_{i+1,j,k} \\
 & + 6 \lambda_{i,j,k}^x u_{i,j,k} - 4 \lambda_{i-1,j,k}^x u_{i-1,j,k} + \lambda_{i-2,j,k}^x u_{i-2,j,k} ], \quad (10)
 \end{aligned}$$

where  $\lambda^x$  is the maximum characteristic speed along the  $x$  axis, and analogous formulae hold for the  $y$  and  $z$  axes.

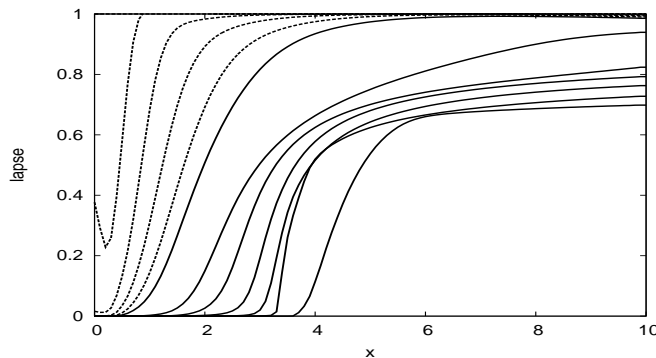


**Figure 2.** Lapse evolution in a 3D black hole simulation (zero shift). The dotted line profiles are plotted every 1M. The solid line ones are plotted every 5M, up to 35M, before boundary-related features become too important (the boundary is just at 10M).

Let us consider initial data taken from a Schwarzschild black hole

$$ds^2 = -\alpha^2 dt^2 + \left(1 + \frac{M}{2r}\right)^4 \delta_{ij} dx^i dx^j. \quad (11)$$

(isotropic coordinates). We will use the 'stuffed black hole' approach (Arbona et al 1998), by matching a scalar field interior metric to (11) (the scalar field will also evolve). As gauge conditions we choose a singularity-avoidant slicing of the '1+log' type in normal coordinates (zero shift).

We present in (Fig. 2) a low-resolution simulation ( $\Delta x = 0.1M$ ) which proves the performance of our numerical method in 3D strong-field scenarios. Even in presence of steep gradients, the lapse profiles evolve smoothly.

The numerical tests shown here have been performed with the Z3 evolution system (first order in space and time) written in a flux conservative form (Bona *et al* 1989). The time integration is dealt by the well-known method-of-lines, with a third-order Runge-Kutta algorithm.

### Acknowledgements

This work has been supported by the Spanish Ministry of Science and Education, through FPI and FPU fellowships and the research grant FPA2004-03666, and by the Balearic Conselleria d'Economia Hissenda i Innovació through the grant PRDIB-2005GC2-06.

### References

- Alcubierre, M. *et al* 2004, *Class. Quantum Grav.*, 21(2), 589613.  
 Alic, D., Bona, C., Bona-Casas, C., Masso, J., 2007, *Phys. Rev. D* 76, 104007.  
 Arbona, A. *et al* 1998, *Phys. Rev. D* 57, 2397.  
 Bona, C., Masso, J., 1989, *Phys. Rev. D* 40, 1022.  
 Gustafson, B., Kreiss, H.O., Olinger, J., 1995, *Time dependent problems and difference methods*, Wiley, New York.